

Coherent Single Charge Transport in Molecular-Scale Silicon Nanowires

Zhaohui Zhong,^{†,§} Ying Fang,^{†,§} Wei Lu,[†] and Charles M. Lieber^{*,†,‡}

Department of Chemistry and Chemical Biology, Harvard University, 12 Oxford Street, Cambridge, Massachusetts 02138, and Division of Engineering and Applied Sciences, Harvard University, Cambridge, Massachusetts 02138

Received April 26, 2005

ABSTRACT

We report low-temperature electrical transport studies of chemically synthesized, molecular-scale silicon nanowires. Individual nanowires exhibit Coulomb blockade oscillations characteristic of charge addition to a single nanostructure on length scales up to at least 400 nm. Studies also demonstrate coherent charge transport through discrete single particle quantum levels extending across whole devices, and show that the ground-state spin configuration is consistent with the constant interaction model. In addition, depletion of nanowires suggests that phase coherent single-dot characteristics are accessible in the few-charge regime. These results differ from those for nanofabricated planar silicon devices, which show localization on much shorter length scales, and thus suggest potential for molecular-scale silicon nanowires as building blocks for quantum and conventional electronics.

Studies of carbon nanotubes¹ and semiconductor nanowires² have demonstrated their potential as building blocks for nanoscale electronics. An advantage of these building blocks versus nanostructures fabricated by “top-down” processing is that the critical feature sizes are defined during synthesis, and thus can be well-controlled at the atomic scale. Indeed, isolated carbon nanotube transistors have shown exceptional properties,³ although difficulties in preparing pure semiconductor nanotubes make large scale integration challenging. Silicon nanowires (SiNWs) could overcome issues faced by carbon nanotubes because current growth methods enable reproducible control over both size and electronic properties of the nanowires.^{4–7} Nevertheless, studies of the fundamental transport properties of SiNWs have not been reported, and thus their potential has remained largely speculative. Recent studies have begun to elucidate detailed transport properties of chemically synthesized semiconducting nanowires,^{8–10} although in these studies the nanowire diameters are typically several tens of nanometers and charge transport is not truly one-dimensional (1D). Molecular-scale silicon nanowires with diameters as small as 3 nm have been reported^{4,5} and are expected to show 1D carrier transport properties due to strong confinement. In this letter we address the fundamental electrical properties of these molecular-scale SiNWs through low-temperature transport measurements of nanowire devices configured as single-electron transistors (SETs).

Single-crystal p-type SiNWs with crystalline core diameters of 3 to 6 nm were synthesized by gold nanocluster mediated vapor–liquid–solid growth using silane and diborane, and devices based on individual SiNWs were fabricated on oxidized silicon substrates using electron beam lithography.^{4,5,11} Current (I) versus gate voltage (V_g) data recorded with a 0.5 mV source-drain bias (V_{sd}) at 4.2 K from a device with source-drain separation of 400 nm exhibit regular oscillations in I over a broad range of V_g as shown in Figure 1a. The current peaks are separated by regions of zero conductance with an average peak-to-peak separation of 0.015 ± 0.001 V. The heights of the observed peaks vary with V_g , although this variation has no obvious periodicity, whereas the position and heights of the peaks are very reproducible on repeated V_g scans in this and similar devices. These observations indicate that the results are intrinsic to transport through the SiNWs, and moreover, are consistent with Coulomb blockade (CB) phenomena resulting from single-charge tunneling through a single quantum structure (e.g., the SiNW) with discrete energy levels.^{12,13} To define better the length-scale of the SiNW structure responsible for the CB oscillations, differential conductance ($\partial I / \partial V_{sd}$) versus V_{sd} and V_g was measured for the device in Figure 1a. These data (Figure 1b) exhibit 33 CB diamonds, where transport is “blocked” for values of $V_{sd} - V_g$ in the light-colored regions. The regular closed diamond structure provides strong evidence for transport through a single quantum structure and not multiple quantum dots (QDs) connected in series, which would exhibit a more complex overlapping diamond structure.¹³ Analysis of these results¹⁴ yields values for the

* Corresponding author. E-mail: cml@cmliris.harvard.edu.

[†] Department of Chemistry and Chemical Biology.

[‡] Division of Engineering and Applied Sciences.

[§] These authors contributed equally to this work.

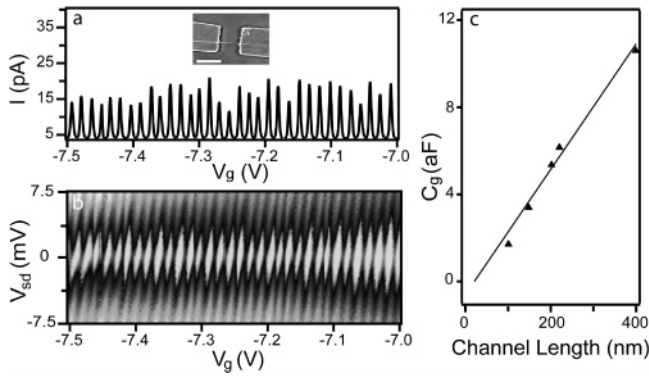


Figure 1. (a) Coulomb blockade oscillations observed at 4.2 K with $V_{sd} = 0.5$ mV. A total of 33 peaks were observed within the 0.5 V sweep of V_g . Inset: scanning electron microscopy (SEM) image of the device. Scale bar is 500 nm. (b) Gray scale plot of $\partial I/\partial V_{sd}$ vs V_{sd} and V_g recorded at 4.2 K; the light (dark) regions correspond to low (high) values of $\partial I/\partial V_{sd}$; the dark color corresponds to 3000 nS. (c) Gate capacitance vs source-drain separation (channel length) for five representative devices showing single-island Coulomb blockade behavior. The line is a fit to the data with a slope of 28 ± 2 aF/ μm .

gate capacitance, C_g , and gate coupling factor, $\alpha = C_g/C$, where C is the total capacitance, of 10.7 aF and 0.33, respectively.

Data exhibiting closed diamonds consistent with transport through single QDs were obtained on small-diameter SiNW devices with source-drain separations ranging from ca. 100 to 400 nm. Importantly, these data show that C_g scales linearly with source-drain separation (Figure 1c), and moreover, the average value of C_g determined from the data, 28 ± 2 aF/ μm , agrees well with that calculated for a cylinder on plane model.¹⁵ These results support our suggestion that the relevant dot size is defined by source-drain electrodes, since a QD size-scale set by structural variations or dopant fluctuations would give a smaller capacitance value and be independent of the source-drain separation. The gate capacitance does deviate from the estimated value when the channel length is < 100 nm, due to screening from the source/drain electrodes when the channel length becomes comparable to the thickness of the gate dielectric.

In addition, the variations in the current peak height versus V_g in Figure 1a suggest the formation of coherent energy states in the SiNW devices with energy level spacing, ΔE , larger than the thermal energy $k_B T$, where peak heights are determined by the coupling of the individual quantum states to the metal contacts at the Fermi level.¹² To investigate this point further we characterized $\partial I/\partial V_{sd} - V_{sd} - V_g$ at higher resolution for a 3 nm diameter SiNW device with a 100 nm source-drain separation as shown in Figure 2a. The data exhibit well-defined peaks in $\partial I/\partial V_{sd}$ that appear as lines running parallel to the edges of the CB diamonds and consistent with discrete single particle quantum levels extending across the SiNW. Analysis of the data yields ΔE values for the first 6 levels of 2.5, 1.9, 3.0, 2.0, 2.0, and 2.9 meV. These can be compared to ΔE estimated using a 1D hard wall potential: $\Delta E = (N/2)h^2\pi^2/m^*L^2$, where N is the number of holes, m^* is the silicon effective hole mass, and L is the device length. ΔE estimated with this model

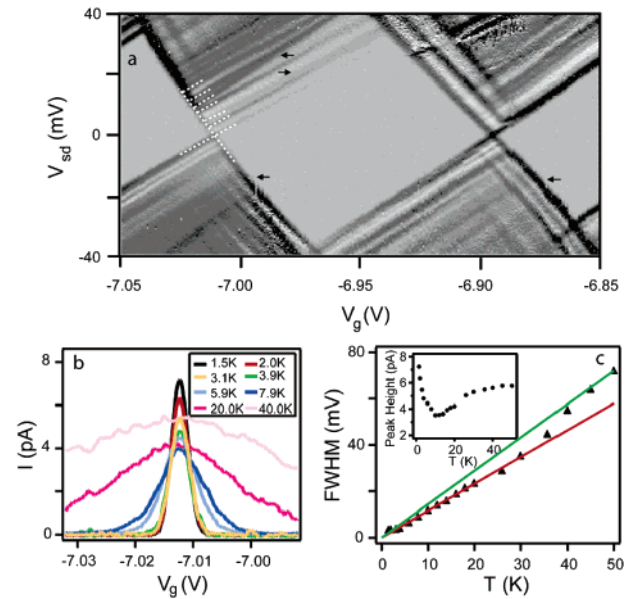


Figure 2. (a) $\partial I/\partial V_{sd} - V_{sd} - V_g$ data recorded at 1.5 K. Dark lines (peaks in $\partial I/\partial V_{sd}$) running parallel to the edges of the diamonds correspond to individual excited states and are highlighted by white-dashed lines. Line slope changes are indicated by black arrows. (b) Temperature-dependent $I-V_g$ curves recorded with $V_{sd} = 50$ μV at increasing temperature. (c) Conductance peak widths in (b) determined from the full-width at half-maximum of the peak height, vs temperature. Solid lines correspond to theoretical predictions for peak widths vs temperature in quantum regime ($\Delta E > k_B T$), $\alpha W = 3.52e k_B T$ (red), and classical regime ($\Delta E < k_B T$), $\alpha W = 4.35e k_B T$ (green), with $\alpha = 0.26$. Inset: temperature dependence of the conductance peak height.

($N \approx 25$,¹⁶ $m^* = 0.39 m_e$,¹⁷ $L = 100$ nm), 2.5 meV, agrees reasonably well with the observed values. Similar results have been observed at 1.5 K in more than 10 SiNW devices with source-drain separations up to 200 nm, and thus we believe it is a robust feature of the small diameter SiNW devices. We also note that the subband spacing for these small diameter SiNWs, ~ 300 meV, is 2 orders of magnitude larger than the level spacing and one order larger than the Fermi energy.¹⁸ Hence, charge transports at 4.2 K involves only the first subband, and the molecular-scale SiNWs are truly 1D.

Temperature dependent $I-V_g$ measurements of the conductance peaks were also carried out. The representative data in Figure 2b show that peak current decreases rapidly as the temperature is increased from 1.5 to 10 K and is approximately constant above 30 K, consistent with coherent tunneling through a discrete SiNW quantum level that is resonant with the Fermi level of the metal contacts.^{12,13} Moreover, the temperature at which the peak becomes constant, 30 K, yields an estimate of $\Delta E \approx 3$ meV that agrees with the value determined from the data and 1D model (see above). In addition, the temperature dependence of the conductance peak width (W) is related to the gate coupling factor, α , as $\alpha W = 3.52k_B T/e$ in the quantum regime, $k_B T < \Delta E$, and as $\alpha W = 4.35k_B T/e$ in the classical regime, $\Delta E < k_B T < U$.¹² Notably, the value of α determined from the temperature dependent data, 0.26, is consistent with that

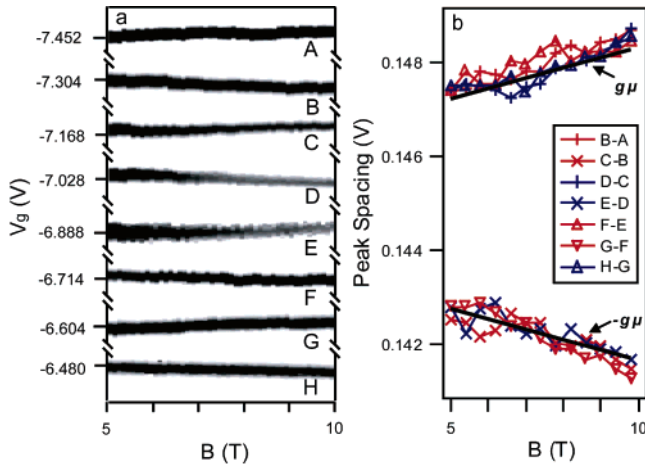


Figure 3. (a) Gray scale plot of I as a function of V_g and parallel magnetic field B at 1.5 K. Data taken from the same device in Figure 2 at different cooling cycle. (b) Peak spacings from (a), offset to align into two branches. Solid black lines indicate expected B-dependence for spin transition from $1/2$ to $-1/2$ (upward), and from $-1/2$ to $1/2$ (downward).

(0.26) obtained directly from Figure 2a, and thus further supports our interpretation of these experiments.

Coherent transport through a single island over length scales of several hundred nanometers indicates that these synthesized SiNWs are clean systems with little/no structural/dopant variation. Indeed, high-resolution transmission electron microscopy shows that the SiNWs have a roughness of only ca. 1–2 atomic layers on the 100 nm scale, which is much less than that produced during the lithographic processing used to define the widths of NWs in planar substrates. We speculate that dopant introduced during nanowire growth also may be driven to the surface of these molecular scale SiNWs as reported for semiconductor nanocrystals.¹⁹ In contrast, low-temperature studies of nanowires with widths as small as ca. 10 nm fabricated by lithography on doped silicon-on-insulator substrates have been interpreted in terms of serially connected quantum dots arising from variations in the potential due to structural and/or dopant fluctuations that are intrinsic to these fabricated structures.^{20,21} The length scale of the electronically distinct regions in these fabricated nanowires is on the order of 10 nm, and thus more than an order of magnitude smaller than 200–400 nm lengths in our 3–6 nm diameter SiNWs.

Clean 1D systems offer unique platforms to study interactions in low-dimension systems. For example, the ground-state (GS) of QDs defined in carbon nanotubes²² was found to have the lowest possible spin, while recent studies on QDs defined in two-dimensional electron gas (2DEG) showed that higher-spin ground states might also be possible.²³ The GS spin states of the SiNW devices were studied with magnetic field parallel to the nanowire axis to minimize orbital effects. Figure 3a shows the gray scale plot of I as a function of V_g and magnetic field B taken from the same device as in Figure 2. A small bias voltage (0.1 mV) was used so that only the ground states contribute to transport. According to the constant interaction model, the GS spin should alternate between $S = 0$ and $S = 1/2$. As a result, the addition energy

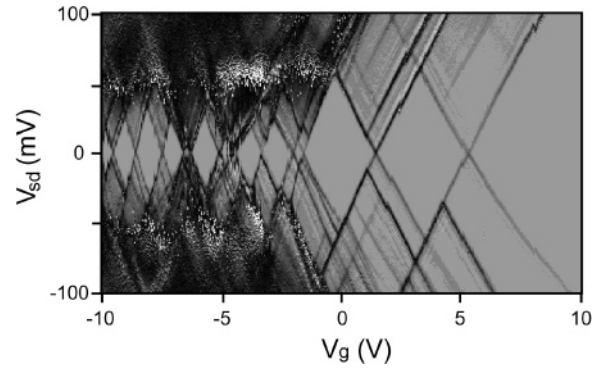


Figure 4. $\partial I/\partial V_{sd} - V_{sd} - V_g$ in gray scale for a SiNW device with 50 nm channel length at 4.2 K. The carriers are completely depleted for $V_g > 5.5$ V.

as measured by CB peak position will exhibit opposite slopes for adjacent peaks as governed by the Zeeman term, $-g\mu_B B \Delta S_z$, with ΔS_z alternating between $1/2$ and $-1/2$ for adjacent charge states.^{22,23} Indeed, data taken from eight consecutive charge states appear as four down–up pairs, as shown in Figure 3a. The slope of the peak positions as a function of magnetic field is in consistent with the Zeeman term, giving an average g value of 2.0 ± 0.2 , which agrees with the bulk Si value.²⁴ Furthermore, peak spacings extracted from the data in Figure 3a are clearly divided into two branches (Figure 3b): an upward branch with slope of $g\mu$ corresponding to transition from spin $1/2$ to $-1/2$ states, and a downward branch with slope of $-g\mu$ corresponding to transition from spin $-1/2$ to $1/2$ states. We did not observe a middle branch, which would be indicative of higher ground-state spin configurations, similar to the observation of carbon nanotubes.²² Furthermore, the simple GS spin configuration also suggests that degeneracy between heavy and light holes is lifted, due to both strain and confinement effects.

The SiNW transport data also exhibit features not explained by the constant interaction model, which we highlight in Figure 2a with arrows. Specifically, we find that transition lines representing ground and excited states can show different slopes, indicating that their gate coupling factors α are different. Bends and kinks within single transition lines show both positive and negative curvature, suggesting that α is not constant for a single level. Similar behavior has been observed in carbon nanotube QDs, and was attributed to either resonant defects or the many-body effect.^{25,26} The positive and negative slope changes seen in our data contrast expectations for the model involving resonant defects²⁵ and may indicate the presence of charge–charge correlation (where C_g is dependent on the device geometry and the many-body states), although future studies will be required to address this interesting point unambiguously.

Last, we have characterized the transport properties of SiNW QDs as they are fully depleted to investigate further the possibility of carrier–carrier correlations in this 1D system. Representative $\partial I/\partial V_{sd} - V_{sd} - V_g$ data recorded on a 50 nm long 3 nm diameter device are shown in Figure 4. Near $V_g = 5.5$ V, the first carrier was added to the dot. Transport is absent at more positive gate voltages, demonstrating that SiNW was fully depleted. There are several

interesting features exhibited by the data in this few charge regime. First, the closed diamonds show that transport is through a single quantum structure, although the variation of diamond size, which is a measure of the minimum energy to add or remove a charge, shows substantially larger variation than data recorded in Figure 1b where there are ca. 800 carriers on the SiNW QD. This variation in charging energy suggests that the CI model is inadequate to treat the few-charge regime and that correlation may lead to shell filling, as observed previously in other QD systems.²⁷ Second, these data also show coherent tunneling through discrete SiNW quantum levels with typical level spacing of several meV. The transition lines exhibit slope changes that are more pronounced than discussed above in Figure 2a and provide further evidence for possible charge–charge correlations. While a quantitative understanding of these observations is not yet in hand, our preliminary results are nevertheless important in demonstrating the possibility of coherent transport to the few-charge regime and should stimulate further experimental and theoretical studies needed to understand better these interesting data.

In conclusion, we have demonstrated that molecular-scale SiNWs can exhibit resonant tunneling at low-temperatures through discrete coherent quantum levels over length scales up to at least 200 nm. These low-temperature results exceed expectations based on many previous studies of lithographically patterned nanowires in planar silicon, and thus point to substantial advantages of silicon-based nanowires prepared by direct synthesis versus top-down approaches for applications in nanoscale electronics. In addition, fundamental studies of 1D SiNWs should serve as an interesting comparison both to carbon nanotubes and quantum wires defined in ultraclean III–V systems. Along these lines, our initial investigations of transport through molecular-scale SiNWs in the few-charge regime demonstrate rich behavior beyond the constant interaction model and could serve as a good test bed for investigating correlation effects and the potential of this system as a building block for quantum electronics.

Acknowledgment. We thank H. Park, C. Marcus, W. Liang, S. Datta and S. Hareland for helpful discussion. C.M.L. is grateful for support of this work by the Defense Advanced Research Projects Agency, Intel, ARO, and NSF.

References

- (1) McEuen, P. L.; Fuhrer, M. S.; Park, H. *IEEE Trans. Nanotechnol.* **2002**, *1*, 78.
- (2) Lieber, C. M. *MRS Bull.* **2003**, *28*, 486.
- (3) Javey, A.; Guo, J.; Wang, Q.; Lundstrom, M.; Dai, H. *Nature* **2003**, *424*, 654.
- (4) Cui, Y.; Lathon, L. J.; Gudiksen, M. S.; Wang, J.; Lieber, C. M. *Appl. Phys. Lett.* **2001**, *78*, 2214.
- (5) Wu, Y.; Cui, Y.; Huynh, L.; Barrelet, C. J.; Bell, D. C.; Lieber, C. M. *Nano Lett.* **2004**, *4*, 433.
- (6) Cui, Y.; Lieber, C. M. *Science* **2001**, *291*, 851.
- (7) Cui, Y.; Zhong, Z.; Wang, D.; Wang, W. U.; Lieber, C. M. *Nano Lett.* **2003**, *3*, 149.
- (8) De Franceschi, S.; Van Dam, J. A.; Bakkers, E.; Feiner, L. F.; Gurevich, L.; Kouwenhoven, L. P. *Appl. Phys. Lett.* **2003**, *83*, 344.
- (9) Thelander, C.; Mårtensson, T.; Björk, M. T.; Ohlsson, B. J.; Larsson, M. W.; Wallenberg, L. R.; Samuelson, L. *Appl. Phys. Lett.* **2003**, *83*, 2052.
- (10) Björk, M. T.; Thelander, C.; Hansen, A. E.; Jensen, L. E.; Larsson, M. W.; Wallenberg, L. R.; Samuelson, L. *Nano Lett.* **2004**, *4*, 1621.
- (11) Single-crystal silicon nanowires were prepared with SiH₄: B₂H₆ ratio of 8000: 1 using 5 nm diameter gold nanocluster catalysts. Devices were fabricated on degenerately doped silicon substrates with 50 nm thermal oxide using electron-beam lithography and subsequent evaporation of 50 nm Ni to define source-drain contacts; devices were annealed at 350 °C for 20 s.
- (12) Grabert, H.; Devoret, M. H. *Single Charge Tunneling: Coulomb Blockade Phenomena in Nanostructures*; Plenum: New York, 1992.
- (13) Kouwenhoven, L. P.; Marcus, C. M.; McEuen, P. L.; Tarucha, S.; Westervelt, R. M.; Wingreen, N. S. in *Mesoscopic Electron Transport*; Sohn, L. L., Kouwenhoven, L. P., Schön, G., Eds.; Kluwer: Dordrecht, 1997.
- (14) The energy to add a charge onto the SiNW, $U+\Delta E$, is directly measured from the maximum in V_{sd} for the conductance gap of the diamond, where $U = e^2/C$ is the charging energy; the addition energy determined from Figure 1b is around 5 meV. The peak spacing ΔV_g is related to the addition energy by $\Delta V_g = (U+\Delta E)/e\alpha$. Assuming that ΔE is small compared to U yields values of $C_g = e/\Delta V_g \approx 10.7$ aF and $\alpha = 0.33$.
- (15) Martel, R.; Schmidt, T.; Shea, H. R.; Hertel, T.; Avouris, Ph. *Appl. Phys. Lett.* **1998**, *73*, 2447.
- (16) The number of carriers were estimated from the difference in V_g required to deplete fully the device (ca. -4 V) and that of the measurement (~ -7 V) using $N = C_g \Delta V_g/e$. For specific parameters in Figure 2a, $N \approx 25$.
- (17) Green, M. A.; *J. Appl. Phys.* **1990**, *67*, 2944.
- (18) The subband energy level spacing, E_n , was estimated using a model with a hard wall potential, $E_n = \hbar^2 \pi^2 n^2 / 2m^* w^2$, where n is the subband number, m^* is the effective mass, and w is the nanowire diameter. For the 3 nm diameter nanowires and $m^* = 0.39 m_e$,¹⁵ the spacing between $n = 1$ and 2 is 320 meV. The Fermi energy, E_F , in 1D is given by $E_F = (Nh/4)^2$, where N is the density of charges per unit length. For typical value of N at 4.2 K, 25/100 nm, $E_F = 15$ meV, implying that only the first subband is occupied.
- (19) Mikulec, F. V.; Kuno, M.; Bennati, M.; Hall, D. A.; Griffin, R. G.; Bawendi, M. G. *J. Am. Chem. Soc.* **2000**, *122*, 2532.
- (20) Tilke, A.; Blick, R. H.; Lorenz, H.; Kotthaus, J. P. *J. Appl. Phys.* **2001**, *89*, 8159.
- (21) Altbauer, T.; Ahmed, H. *Jpn. J. Appl. Phys.* **2003**, *42*, 414.
- (22) Cobden, D. H.; Bockrath, M.; McEuen, P. L.; Rinzler, A. G.; Smalley, R. E. *Phys. Rev. Lett.* **1998**, *81*, 681.
- (23) Folk, J. A.; Marcus, C. M.; Berkovits, R.; Kurland, I. L.; Aleiner, I. L.; Altshuler, B. L. *Phys. Scripta* **2001**, *T90*, 26.
- (24) Feher, G.; Hensel, J. C.; Gere, E. A. *Phys. Rev. Lett.* **1960**, *5*, 309.
- (25) Cobden, D. H.; Nygård, J. *Phys. Rev. Lett.* **2002**, *89*, 046803.
- (26) Tans, S. J.; Devoret, M. H.; Groeneveld, R. J. A.; Dekker, C. *Nature* **1998**, *394*, 761.
- (27) Kouwenhoven, L. P.; Oosterkamp, T. H.; Danoesastro, M. W. S.; Eto, M.; Austing, D. G.; Honda, T.; Tarucha, S. *Science* **1997**, *278*, 1788.

NL050783S